Current Programmed Mode Control of Multi-Level Flying Capacitor Converter Near Zero-Ripple Current Region

Liangji Lu, Aleksandar Prodić
Laboratory for Power Management and Integrated SMPS
ECE Department, University of Toronto
Toronto, ON, CANADA
liangji.lu@mail.utoronto.ca, prodic@ece.utoronto.ca

Giacomo Calabrese, Giovanni Frattini, Maurizio Granato
Texas Instruments
Freising, GERMANY and Milan, ITALY
{g-calabrese,giovanni.frattini,maurizio.granato}
@ti.com

***Abstract*— This paper explores the challenges and introduces a solution for near zero-ripple current region operation of multi-level flying capacitor (ML-FC) converters, operating in peak and valley current programmed mode (CPM). Around the zero-ripple region, the triangular inductor current ripple waveform is modified to be trapezoidal using a state machine. Seamless transition between peak and valley is desirable to ensure symmetrical stable operation below and above the duty-cycle yielding zero-ripple current. In both cases, flying capacitor voltage inherent stabilization is achieved. The investigated ideas are verified with a three-level FC buck converter with 5 V output operating at 500 kHz nominal switching frequency near 50% duty-cycle, the zero-ripple current region.**

Keywords*— *multi-level flying capacitor (ML-FC) converters, zero-ripple current region, cpm control, flying capacitor voltage balancing

I. INTRODUCTION

Multi-level flying capacitor (ML-FC) converters [1]-[3], have been increasingly investigated in low power dc-dc applications, processing from a fraction of watt to few kilowatts, as an alternative to predominantly used conventional two-level buck and boost converters. This is mostly due to potential for improving power processing efficiency while reducing physical size [4]-[5], which is highly attractive for the targeted cost sensitive volume constrained applications. However, several control challenges, specific to the targeted low-power dc-dc application [6]-[8], have hindered a wider adoption of ML-FC converters. One of those is practical implementation of peak current programmed mode (CPM) control that, due to features such as inherent current protection and simplified system dynamics [9], is widely used with conventional topologies. Specific challenges include regulation of the flying capacitor (FC) voltage and operation of the CPM controllers around zero-current ripple region. Recent literature has been investigating FC control challenges and solutions for various control methods have been presented, including those for voltage mode [6]-[8], peak current mode [10], valley current mode [11]-[13], and average current mode [14]. In [6], voltage spikes related problems at zero current ripple operating points that, unlike for the conventional buck, for ML-FC occurs not only for the extreme values of voltage conversion ratios, i.e. $M(D) = 0$ and $M(D) = 1$, but also at other points, have been addressed and a solution for its elimination presented.

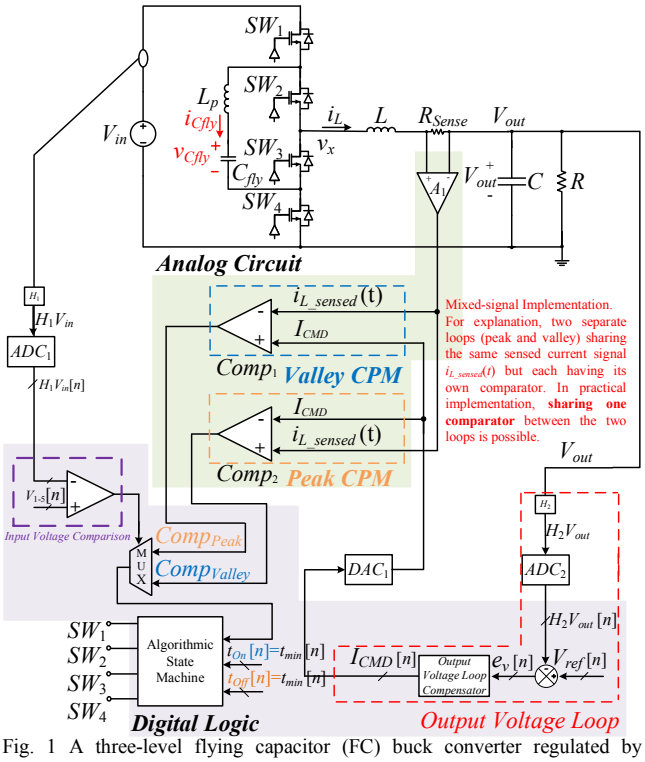

Fig. 1 A three-level flying capacitor (FC) buck converter regulated by peak/valley CPM controller that provides regulation around zero ripple operating points.

This paper addresses the problem of loss of regulation in peak and valley CPM control around zero current ripple operating points, naturally related to the loss of the carrier signal for pulse-width modulation, i.e. loss of ripple, and introduced a solution for the same. The introduced controller, shown in Fig.1, utilizes the concept of a trapezoidal current waveform modulation [6] around zero-ripple operating point that not only provides tight output voltage regulation but also eliminates voltage spike problems occurring at that point, while maintaining inherent stabilization of the flying capacitor voltage, $v_{cfly}(t)$. Furthermore, the controller provides a seamless

This work of Laboratory for Power Management and Integrated SMPS is supported by Texas Instruments.

transition between peak and valley trapezoidal modulations to cover symmetrical stable operation below and above the duty-cycle yielding zero-ripple. The investigation is divided into three sections. First, peak and valley-based CPM control will be discussed with modulation scheme resulting in equivalent trapezoidal inductor current waveform shown in [6]; and the seamless transition between the two modes will be in essence to cover symmetrical stable operation above/below 50% duty-cycle. In both cases, v_{Cfly} stabilization can be inherently achieved. Second, algorithmic state machine implementation of the controller will be demonstrated. Finally, experimental results will be shown to effectively demonstrate the control concepts discussed.

.

II. Near Zero Current Ripple Region in Peak and Valley CPM Control

This section addresses the problems of voltage spikes and the loss of carrier signal for the peak or valley CPM operating around zero-current ripple and reviews the concept of trapezoidal current modulation for eliminating the spikes. Then, the operation of the introduced peak/valley CPM controller and inherent FC voltage stabilization is explained using the example of the three-level FC buck converter of Fig.1.

Fig.2 shows the key open-loop waveforms of a three-level buck operating away from the zero-ripple operating point (dashed lines) and at the zero-ripple point (solid lines), for $M(D) < 0.5$. While operation away from the zero-ripple, there are three distinct current slopes (m_1, m_2, and m_3) determined by V_{in}, V_{cfly}, and V_{out}. Ideally, in steady-state, v_{Cfly} should be equal to $V_{in}/2$, i.e. a half of the input voltage, resulting in $m_1 = m_3$ and the switching node, v_x, switching between 0 and $V_{in}/2$ (or between $V_{in}/2$ and V_{in} for $M(D) > 0.5$). The inductor current waveform is similar to that of a conventional buck and, ideally, a standard peak CPM controller [9] could regulate the output voltage. However, as shown in Fig.3 demonstrating dependence of the ripple amplitude Δi_L on $M(D)$ [6], for some conversion ratios, the ripple that, for peak and valley CPM is the key signal (carrier) for forming the pulse-width modulated control signal, diminishes and for $M(D) = 0.5$ becomes zero. Therefore, straightforward implementation of a peak or valley CPM becomes impossible. Fig. 2 shows that at $M(D) = 0.5$, the time interval between C_{fly} charging and discharging becomes zero, eliminating the time needed for the relaxation of the energy stored in the FC equivalent series inductance of L_p (Fig.1). In [6], it was shown that this lack of relaxation time causes destructive voltage spikes and a solution for voltage mode control, based on trapezoidal modulation of the inductor current, which skips the critical point, was introduced.

A. Valley CPM Operation for Trapezoidal Inductor Current Waveform

The modulation of the trapezoidal inductor current waveform shown in [6] solves for the problem of destructive voltage spikes, described in the previous subsection. It also, results in a non-zero ripple amplitude, allowing for potential

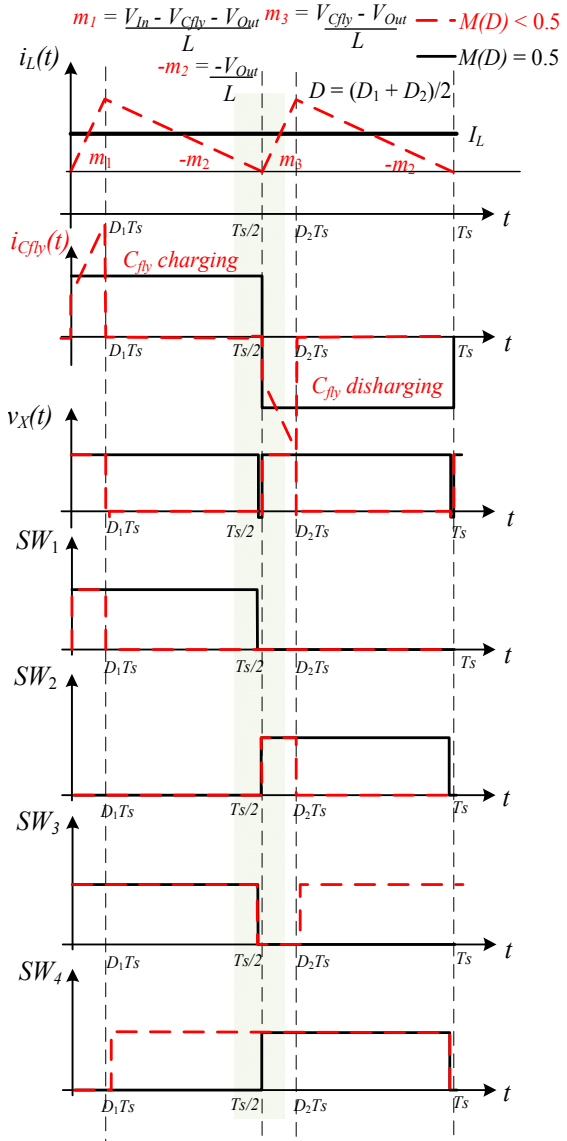

Fig. 2 Steady-state waveforms of a three-level FC buck converter for $M(D) < 0.5$ (dashed line) and for $M(D) = 0.5$ (solid line). Top to Bottom: $i_L(t)$, $i_{Cfly}(t)$, Switching node voltage, $v_x(t)$, *and gating signals for* SW_1 to SW_4.

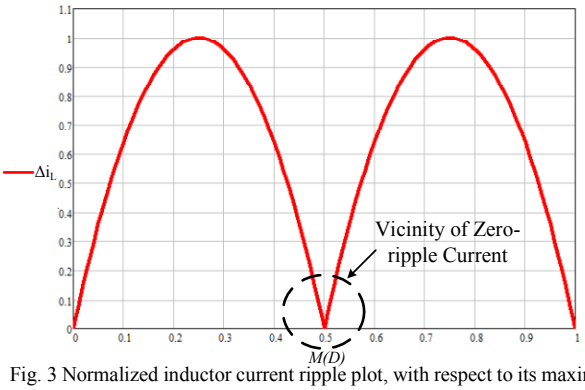

Fig. 3 Normalized inductor current ripple plot, with respect to its maximum value, against the conversion ratio for a three-level FC buck converter.

peak or valley CPM controller implementation. However, direct utilization of that concept is not possible, since it relies on the duty-cycle information, which is not directly accessible in peak and valley-based CPM control techniques.

The solution introduced here enables implementation of peak/valley CPM control around zero-ripple region and eliminates the voltage spikes by utilizing previously introduced trapezoidal modulation concept [6] and modifying it for CPM modulation. The trapezoidal current produced by this controller for $M(D)$ around 0.5, shown in Fig.4, has a similar waveform to that used in [6] but the way the gating sequence is produced is different. Inductor volt-second balance over two switching periods will yield the result in Eq. (1), and the conversion ratio, $M(D)$, is now a function of t_{On}(v_x connects to V_{in}, peak) and t_{Off}(v_x connects to ground, valley) seen in Eq. (2):

$$< V_{out} >_{2T_S} = (1 + \frac{t_{On} - t_{Off}}{T_S}) \frac{V_{in}}{2} \quad , \qquad (1)$$

$$M(D) = \frac{V_{out}}{V_{in}} = 0.5 + \frac{t_{On} - t_{Off}}{2T_S} \quad , \qquad (2)$$

The two equations indicate that when duty-cycle is exactly at 50%, t_{On} will be equal to t_{Off} ($t_{On} = t_{Off}$), however, if duty-cycle is slightly less than 50%, t_{On} will be less than t_{Off} ($t_{On} < t_{Off}$) meaning the switching node v_x will be connected to ground for a longer duration and vice versa for the case when $M(D) >$ 50%.Thus, by modulating the difference between the two durations t_{On} and t_{Off}, one can achieve the desired $M(D)$ below, equal, or above the 50% duty-cycle. Instead of providing both peak and valley commands at the same time which will involve ripple estimation with more complexed hardware, one of the two parameters t_{On} or t_{Off} can be fixed at a constant value and let the other be controlled by the peak or valley current command to achieve the desired conversion ratio. C_{fly} will be charged and discharged in two alternating pairs within two switching cycles, but one will see in the next sub-section that this pattern will lead to inherent FC voltage stabilization. Considering the operation when $M(D)<$ 50%, t_{On} is fixed to be a constant value, and only control the valley point to modulate the t_{Off} parameter and obtain the desired $M(D)$ as shown in Fig.5. The current ripple now is defined as

$$\Delta i_{L\_ValleyModulation} = \frac{V_{in} D}{L} (1 - 2D + {t_{On}}/{T_S}) T_S \quad , \qquad (3)$$

One can see that when $M(D)$ = 0.5, the current ripple is raised above 0, and the magnitude will be directly proportional to t_{On}; however, the current ripple should be raised but at a minimum value above 0 such that it does not drastically affect the converter efficiency, the constant t_{On} is then selected to be the minimum on-time of the converter t_{min} which is determined by the deadtime setting, switch turn-on delay, as well as the minimum turn-on time of the switch to achieve the minimized ripple near $M(D) = 0.5$ in this modulation. There is a total of eight switching states within every two-switching cycle as shown in Fig.4. Fig.5 illustrates the operation where duty-cycle is slightly less than 50%; t_{On} is fixed at t_{min}, and one observes that $t_{On} < t_{Off}$; slopes in state 2, 4, 6, and 8 will be greater than 0. For the case where duty-cycle is slightly greater than 50%, $t_{On} > t_{Off}$, and the four slopes will be less than 0.

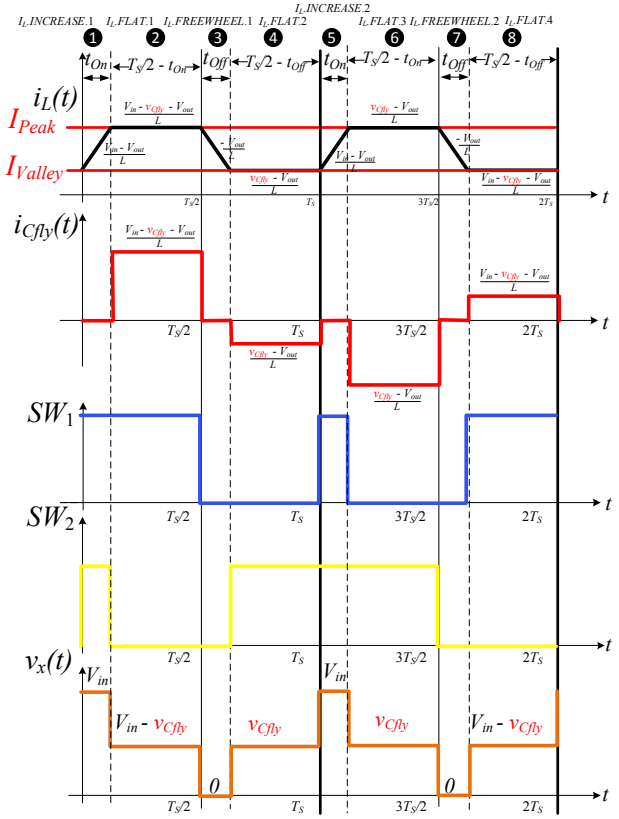

Fig. 4 Steady-state waveforms when duty-cycle equals to 50% using trapezoidal current modulation in peak and valley CPM. Top to Bottom: $i_L(t)$, $i_{Cfly}(t)$, *gating signals for* SW_1 *and* SW_2, and $v_x(t)$.

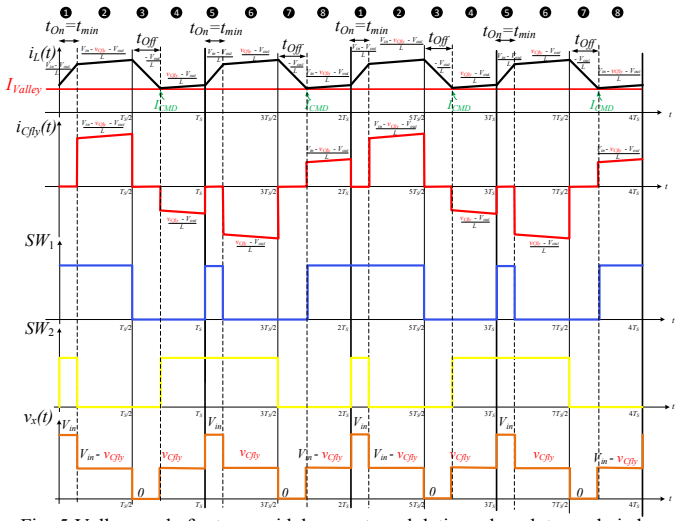

Fig. 5 Valley mode for trapezoidal current modulation when duty-cycle is less than 50% with t_{On} fixed at t_{min}. Top to Bottom: $i_L(t)$, $i_{Cfly}(t)$, *gating signals for* SW_1 *and* SW_2, and $v_x(t)$.

B. Valley Modulation Challenge and Peak Modulation

Since the zero-ripple region exists within a range from below to above 50% duty-cycle operation, the modulation scheme should be designed to ensure smooth operation along the entire range above and below 50%. However, as t_{On} is fixed at t_{min} to obtain minimized current ripple in this modulation, t_{Off} (state 3 and 7 in Fig.5) will be shortened gradually as the conversion ratio goes above 50%; at $M(D) = (0.5+t_{min}/T_S)$, t_{Off} will need to be 0 to achieve this effective duty-cycle which is not desirable due to deadtime constraint. Thus, symmetrical range of above and below 50% duty-cycle in the zero-ripple current region will not be achievable utilizing only valley mode control. However, peak mode will be of interest in this case because peak mode will be fixing the t_{Off} parameter at a constant value and giving enough freedom to adjust t_{On} based on the peak command. The current ripple in peak modulation is expressed as:

$$\Delta i_{L\_PeakModulation} = \frac{V_{in}(1-D)}{L}(2D-1+{}^{t_{Off}}\!/_{T_S})T_S \ , \quad (4)$$

When $M(D)$> 50%, t_{On} is the dominant factor and should be larger than t_{Off} in order to achieve the desired duty-cycle (Eq.(2)). By fixing t_{Off} at the minimum, t_{min}, when duty-cycle is greater than 50%, one can use peak command to control the parameter t_{On} accordingly to achieve the desired duty-cycle without violating the deadtime setting and at the same time obtain the minimum current ripple possible in this modulation scheme based on Eq.(4). Peak CPM modulation when duty-cycle is slightly greater than 50% can be seen in Fig.6.

By combining valley and peak modulations near zero-ripple region, based on the current ripple equations in Eqs.(3)-(4), it is possible to achieve the desired normalized current ripple in Fig.7. The mechanism will start acting when $M(D)$ is around $(0.5-t_{min}/T_S)$ into valley mode trapezoidal current modulation till it approaches 0.5; then, peak modulation will be used to cover

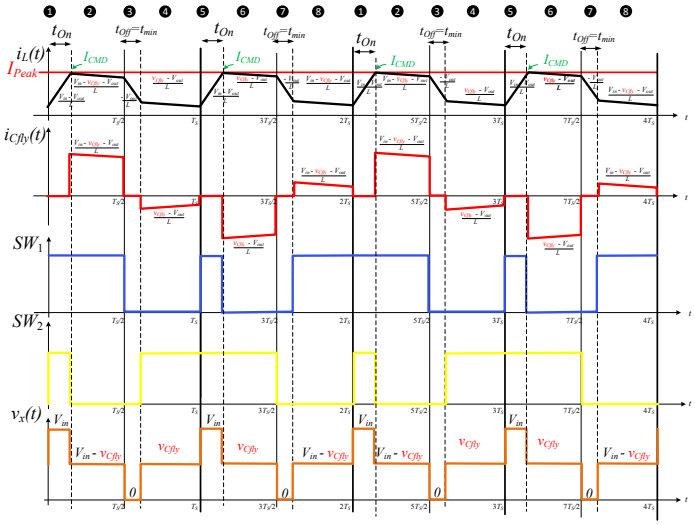

Fig. 6 Peak mode for trapezoidal current modulation when duty-cycle is greater than 50% with t_{Off} fixed at t_{min}. Top to Bottom: $i_L(t)$, $i_{Cfly}(t)$, *gating signals for* SW_1 *and* SW_2, and $v_x(t)$.

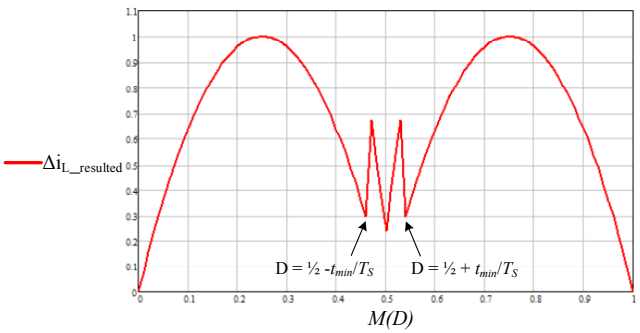

Fig. 7 Normalized inductor current ripple with trapezoidal current modulation scheme near zero-ripple region plot against duty-cycle for a three-level FC buck converter.

up to $M(D) = (0.5+t_{min}/T_S)$; the rest of duty-cycle range will use conventional triangular inductor current waveform.

C. Intrinsic FC Voltage Stabilization Methods

Another important feature in this valley and peak mode trapezoidal modulation near 50% duty-cycle is the intrinsic v_{Cfly} stabilization. In Fig.8.(a), the green line shows the condition where v_{Cfly} is disturbed to be less than its desired voltage, $V_{in}/2$, in valley mode modulation, and the slopes related to v_{Cfly} will be distorted leaving slopes in C_{fly} charging states 2 and 8 to be greater than the slopes in C_{fly} discharging states 4 and 6. The intention is to have a resultant positive charge from each two-switching period to increase v_{Cfly} to reach $V_{in}/2$. As can be seen in Fig.8.(a), without additional v_{Cfly} stabilization mechanism, the slope distortions combined with valley control will leave the charging current in state 2 and 8 to be greater than the discharging current in state 6 and 4, respectively leaving a resultant positive charge. Therefore, the system inherently rejects disturbances. In addition, in peak mode modulation as shown in Fig.8. (b), it still has natural perturbation rejection ability relying mainly on one pair of the charging and discharging sequence of the flying capacitor. Intrinsic v_{Cfly} stabilization can always be guaranteed in peak and valley trapezoidal modulation scheme.

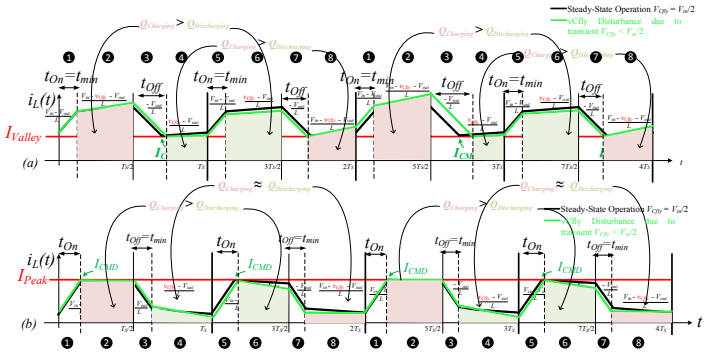

Fig. 8 Key current waveforms of (a). valley mode and (b). peak mode trapezoidal current modulation near zero-ripple region for three-level FC buck in the presence of v_{Cfly} disturbance ($v_{Cfly} < V_{in}/2$).

III. Practical Implementation

As shown in previous section, the optimum operation can be achieved by combining valley and peak modulations at the vicinity of zero-ripple current region. When duty-cycle is less and close to 50%, valley mode modulation is used, and when duty-cycle is close and larger than 50%, peak mode modulation is preferred to ensure stable operation. Therefore, seamless transition between valley to peak and vice versa is required.

A. Algorithmic State Machine

The implementation of the controller utilizes algorithmic state machine (Figs.9-10). Within one effective cycle (consisting of two switching periods) from state 1 to 8, each interval is assigned a state name as shown in Fig.4. Assuming a fixed output voltage, the mode selection is made based on input voltage information with an excessive hysteresis band [15]-[16] implemented to avoid undesirable mode toggling between peak and valley. Depending on which operation mode is currently in, the mode for next cycle will be determined at the very end of the current cycle based on the input voltage information (Figs.9-10).

B. Mixed Signal Implementation

As shown in Fig.1, implementation of this controller is mixed signal. In digital domain, the output voltage loop compares output voltage, V_{out}[n], to a reference, V_{ref}[n], and generate error signal, e_v[n]. Then e_v[n] goes through a compensator and provides the major valley or peak current command depending on which mode the converter is operating in. For demonstration purpose, Fig.1 shows two separate loops for peak and valley mode sharing the same sensed inductor current, i_{L_Sensed}(t), but each having its own comparator; however, in practice, only one comparator is utilized to share between the two loops. On one hand, in valley mode, t_{On}[n] will be a fixed minimum value in state 1 and 5 where the switching node is connecting to V_{in}, and t_{Off}[n] will be determined by the valley command. I_{CMD}[n] which will be converted into an analog signal I_{CMD} using DAC_1 to be compared with the sensed inductor current and obtain the desired duty-cycle. On the other hand, in peak mode, t_{Off}[n] will be fixed at the minimum value in state 3 and 7 where the switching node is connecting to ground, and t_{On}[n] will be determined by the peak command, I_{CMD}[n]. The mode selection will be determined at the very end of state 8 which compares V_{in} to a range of references, $V_{1\text{-}5}$[n], as shown in Fig.9 and 10 and determines which operating mode will be active for the next effective cycle. In addition, this control method can be easily blended into other duty-cycle range of operation using peak and valley-based CPM. Conventional valley CPM for triangular inductor current can be used when V_{in} is less than V_1 in Fig.9, and when V_{in} goes above V_1, trapezoidal inductor current can be generated in valley CPM as discussed in Section II; operation will stay in zero-current ripple valley operation until Vin goes above V_4 where the system will transit into zero-current ripple peak mode operation; then when V_{in} is above V_5, peak CPM for triangular

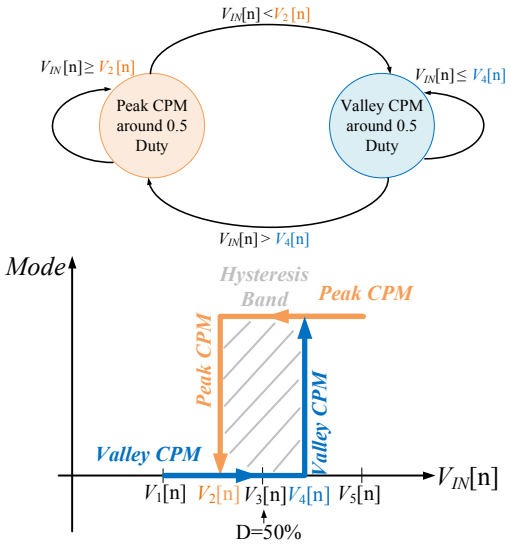

Fig. 9 Algorithmic State Machine for choosing operating mode with Hysteresis band implemented ensuring stable operation.

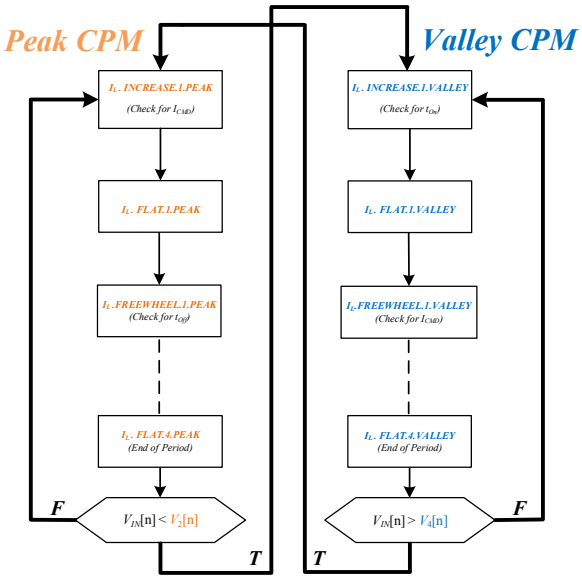

Fig. 10 State diagram for one effective cycle (two switching period) in peak and valley based trapezoidal current modulation scheme.

inductor current can be used. Mode transition from peak to valley at zero-ripple region is based on a similar concept except that the transition will happen at voltage reference V_2 as shown in Fig. 9. The hysteretic band as shown in [15]-[16] is added to eliminate excessive mode toggling problem.

IV. Experimental Results

Experimental prototype was built based on Fig.1. The digital logic was implemented using FPGA and a custom-made discrete control board with discrete analog current sensor, analog comparator, analog-to-digital converters, and digital to analog converters. A three-level 5 V output, 10 W, 500 kHz nominal switching frequency, FC buck prototype was built

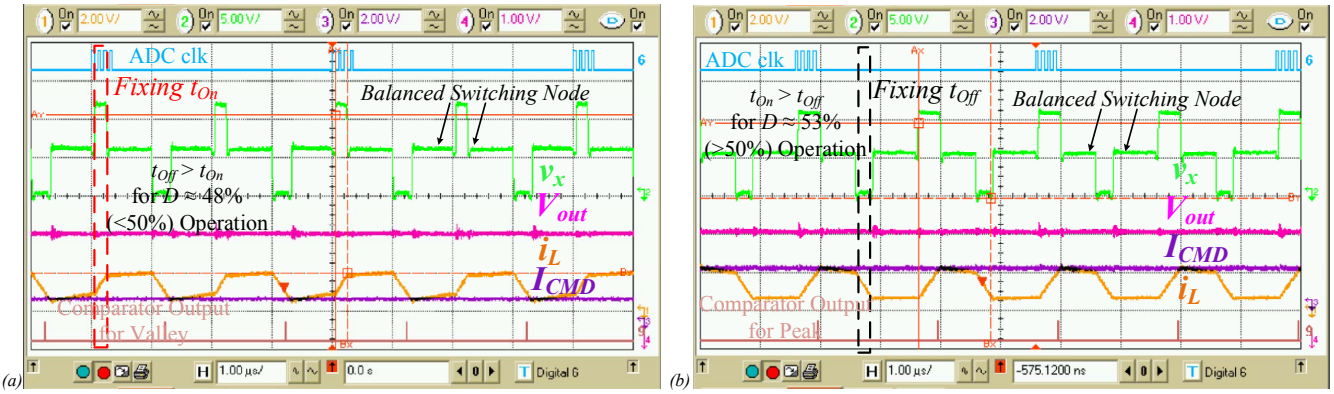

Fig. 11 V_{out} = 5V. *(a)* D ≈ 48% in valley mode modulation, and *(b)* D ≈ 53% in peak mode modulation, near zero-ripple current region. Ch1. 2[V]/div: i_L; Ch2. 5[V]/div: v_x; Ch3. 2[V]/div: I_{CMD}; Ch4. 1[V]/div: V_{out}

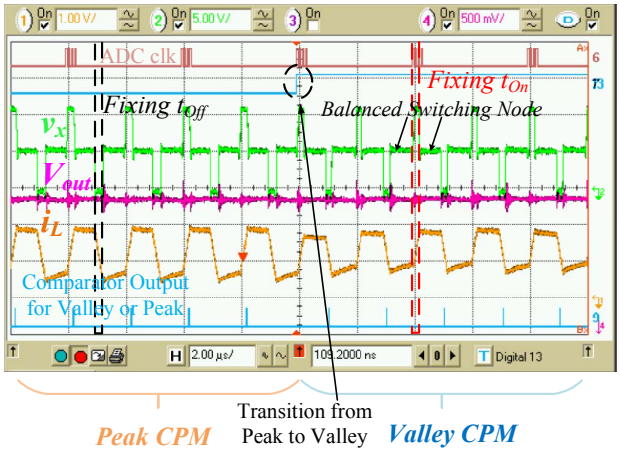

Fig. 12 V_{out} = 5V, mode transition from peak to valley modulation near zero-ripple current region; Ch1.1[V]/div:i_L;Ch2.5[V]/div:v_x;Ch4.500[mV]/div:V_{out}.

operating near the zero-ripple current region where input voltage varies between 9 V to 11V. Fig. 11 shows steady-state operation of valley and peak trapezoidal current modulation near the zero-ripple region. v_{Cfly} can be inherently stabilized at $V_{in}/2$ without additional v_{Cfly} stabilization mechanism as shown in Fig.1. Also, Fig.12 shows example of seamless mode transition from peak to valley confirming stable operation in between the transition boundary.

V. Conclusions

This paper discusses three-level FC buck converter near zero-ripple current region operation in peak and valley CPM. Trapezoidal inductor current waveform is achieved as seen in skip-duty modulation in voltage mode [6] by fixing t_{On} in valley and t_{Off} in peak mode when *M(D)* is below and above 50% respectively with seamless transition implemented using hysteresis band [15]-[16]. In addition, inherent v_{Cfly} stabilization can be achieved in both modulations. The effectiveness of the control scheme is verified through experiments.

References

[1] T.A. Meynard, H. Foch, "Multi-level conversion: high voltage choppers and voltage-source inverters," *in Proc. IEEE PESC* '92, vol. 1. pp.397-403 July 1992.

[2] T.A Meynard, H. Foch, "Multilevel converters and derived topologies for high power conversion," *in Proc. 1995 IEEE 21st Int. Conf. Industrial Electronics, Control, and Instrumentation,* pp. 21–26. Nov. 1995.

[3] T.A. Meynard, H. Foch, P. Thomas, J. Courault, R. Jakob and M. Nahrstaedt, "Multicell converters: basic concepts and industry applications," *IEEE Trans on Industrial Electron*., vol.49, no.5, pp. 955- 964, Oct 2002.

[4] N. Vukadinović, A. Prodić, B. A. Miwa, C. B. Arnold, M. W. Baker., "Volume and Efficiency Comparison Between Multi-level Dc-Dc Converters and Buck Converter for Low-Power Mobile Applications" *18th International Symposium on Power Electronics Ee 2015*, Novi Sad, Serbia, October 2015.

[5] Y. Lei, W.C. Liu and R.C.N. Pilawa-Podgurski, "An Analytical Method to Evaluate Flying Capacitor Multilevel Converters and Hybrid Switched-Capacitor Converters for Large Voltage," *IEEE Workshop on Control and Modeling for Power Electronics (COMPEL)* July 2015.

[6] N. Vukadinovic, A. Prodic, B. A. Miwa, C. B. Arnold and M. W. Baker, "Skip-duty control method for minimizing switching stress in low-power multi-level Dc-Dc converters," in 2015 IEEE 16th Workshop on Control and Modeling for Power Electronics (COMPEL), Vancouver, BC, 2015.

[7] N. Vukadinovic, A. Prodic, B. A. Miwa, C. B. Arnold, and M. W. Baker. "Extended Wide-Load Range Model for Multi-Level DC-DC Converters and a Practical Dual-Mode Digital Controller". In *Proc. 31st Applied Power Electronics Conference and Exposition (APEC 2016)*, March 2016.

[8] Nenad Vukadinovic, Aleksandar Prodic, Brett A. Miwa, Cory B. Arnold, Michael W. Baker, "Discontinuous conduction mode of multi-level flying capacitor DC-DC converters and light-load digital controller", *Control and Modeling for Power Electronics (COMPEL) 2017 IEEE 18th Workshop on*, pp. 1-7, 2017.

[9] R. W. Erickson and D. Maksimović, Fundamentals of Power Electronics.: New York: Springer-Verlag, 2001.

[10] L. Lu, S. M. Ahsanuzzaman, A. Prodic, G. Calabrese, G. Frattini and M. Granato, "Peak offsetting based CPM controller for multi-level

flying capacitor converters," *2018 IEEE Applied Power Electronics Conference and Exposition (APEC)*, San Antonio, TX, 2018, pp. 3102-3107.

[11] D. Reusch, F. C. Lee and M. Xu, "Three Level Buck Converter with Control and Soft Startup," in *2009 IEEE Energy Conversion Congress and Exposition*, San Jose, CA, 2009.

[12] J. S. Rentmeister, C. Schaef, B. X. Foo, and J. T. Stauth, "A flying capacitor multilevel converter with sampled valley-current detection for multi-mode operation and capacitor voltage balancing," *in 2016 IEEE Energy Conversion Congress and Exposition (ECCE)*, Sept 2016.

[13] Jan S. Rentmeister, Jason T. Stauth, "A 48V:2V flying capacitor multilevel converter using current-limit control for flying capacitor balance", Applied Power Electronics Conference and Exposition (APEC) 2017 IEEE, pp. 367-372, 2017, ISSN 2470-6647.

[14] L. Lu, Y.Zhang, S. M. Ahsanuzzaman, A. Prodic, G. Calabrese, G. Frattini and M. Granato, "Digital Average Current Programmed Mode Control for Multi-level Flying Capacitor Converters," *2018 IEEE 19th Workshop on Control and Modeling for Power Electronics (COMPEL)*, Padua, 2018, pp. 1-7.

[15] Y. Zhang *et al*., "Low-frequency ripple-shaping controller for operation of non-inverting buck-boost converters near step-up step-down boundary," *2018 IEEE Applied Power Electronics Conference and Exposition (APEC)*, San Antonio, TX, 2018, pp. 292-297.

[16] Y. Zhang, L. Lu, S. M. Ahsanuzzaman, A. Prodic, G. Calabrese, G. Frattini, and M. Granato. "Multilevel Non-Inverting Buck-Boost Converter with Low-Frequency Ripple-Shaping Based Controller for Operating in Step-down/Step-up Transition Region," *2018 IEEE 19th Workshop on Control and Modeling for Power Electronics (COMPEL)*, Padua, 2018, pp. 1-7.